

Optimal control and management of a large-scale battery energy storage system to mitigate fluctuation and intermittence of renewable generations



Xiangjun LI¹, Liangzhong YAO¹, Dong HUI¹

Abstract Battery energy storage system (BESS) is one of the effective technologies to deal with power fluctuation and intermittence resulting from grid integration of large renewable generations. In this paper, the system configuration of a China's national renewable generation demonstration project combining a large-scale BESS with wind farm and photovoltaic (PV) power station, all coupled to a power transmission system, is introduced, and the key technologies including optimal control and management as well as operational status of this BESS are presented. Additionally, the technical benefits of such a large-scale BESS in dealing with power fluctuation and intermittence issues resulting from grid connection of large-scale renewable generation, and for improvement of operation characteristics of transmission grid, are discussed with relevant case studies.

Keywords Battery energy storage systems, Renewable generations, Power fluctuation, Battery energy management system, Power control

CrossCheck date: 21 September 2016

Received: 3 July 2016/Accepted: 22 September 2016/Published online: 24 October 2016

© The Author(s) 2016. This article is published with open access at Springerlink.com

✉ Xiangjun LI
lixiangjun@epri.sgcc.com.cn

Liangzhong YAO
yaoliangzhong@epri.sgcc.com.cn

Dong HUI
huidong@epri.sgcc.com.cn

¹ State Key Laboratory of Control and Operation of Renewable Energy and Storage Systems, China Electric Power Research Institute, Beijing 100192, China

1 Introduction

Renewable energy power generation has become an important part for China's power supply. By June 2016, the grid's wind-power capacity had been 124 GW and the photovoltaic (PV) capacity had been 61 GW. The rapid development and implementation of renewable power generation pose great challenges to the operation, control, and security of the Chinese power grid. Large-scale battery energy storage system (BESS) can effectively compensate the power fluctuations resulting from the grid connections of wind and PV generations which are random and intermittent in nature, and improve the grid friendliness for wind and PV generation grid integration.

Large-scale BESS can participate in the operation as either the power supply or the load when needed. Unlike traditional power generation systems, BESS can act as a rapid-response active and reactive power injection or absorption device [1–8]. The BESS can be used to smooth the power fluctuations of PV or wind power stations [9–12]. Based on the existing researches and implementations of large-scale BESS worldwide, countries such as the United States, Germany and Japan, have carried out more than 200 demonstration projects. For example, redox flow and sodium sulfur battery is one of the cutting edge technologies for renewable energy power generation applications in Japan [13–15]. There are also more applications of lithium-ion BESS in the United States, such as in the fields of renewable energy generations, distributed generations, micro grids, etc. The American Xtreme Power, Duke Energy, Altairnano, and AES Energy storage companies, for example, have conducted researches on energy storage technologies [16–18]. At present, existing applications of large-scale lithium, sodium-sulfur or redox flow battery have reached to tens of megawatts (MW) in power rating.



However, they are generally used only for wind energy storage or solar energy storage respectively. Although the MW power level of BESS is generally high, the MWh capacity level is relatively low. For example, the BESS of Japan Hokkaido wind farm incorporates a vanadium redox flow BESS with the power capacity 4 MW/6 MWh and is mainly for smoothing the wind power output fluctuations [18–20]. The Japan Aomori Six Village energy storage power station utilizes a sodium sulfur BESS with the power capacity 34 MW, mainly for smoothing the wind power fluctuations [18, 21]. The Texas wind farm storage power station uses an advanced lead-acid battery (36 MW/9 MWh), principally for frequency regulation, energy transfer and peak load shaving [18, 22]. The West Virginia Elkins wind farm energy storage power station incorporates a lithium-ion battery (32 MW/8 MWh) which is for frequency regulation and output climbing control [18, 23].

In China, there are a number of large-scale BESS demonstration projects currently underway. For example, in Zhangbei, a large-scale BESS, which includes a 14 MW/63 MWh lithium-ion BESS and a 2 MW/8 MWh vanadium redox flow BESS, has been put into operation (flow BESS is still in the site commissioning stage). It is part of a national wind, PV, storage and transmission demonstration project. The purpose of this project is to smooth the wind and PV power fluctuations and trace the scheduled power outputs to grid. Further, Guodian Longyuan Woniushi wind farm energy storage power station, using total vanadium flow batteries (5 MW/10 MWh), is adopted mainly to resolve wind-curtailment and brownout issues arising at the Woniushi wind farm. The BESS of Southern Power Grid Shenzhen Baoqing adopted the lithium-ion battery (planned capacity is 10 MW and completed capacity is 4 MW/16 MWh) to achieve peak load shaving, frequency regulation, and voltage regulation, etc.

In this paper, the system configuration of a national renewable generation demonstration project, combining a large-scale BESS with wind farm and PV power station all coupled to a power transmission system, is introduced, and the key technologies and operational status of this BESS are presented. Additionally, the technical benefits of such a large-scale BESS in dealing with power fluctuation and intermittence issues resulting from grid connection of large-scale renewable generation, and for improvement of operation characteristics of transmission grid, are discussed with relevant case studies.

2 Large battery energy storage station in Zhangbei

The Zhangbei energy storage power station is the largest multi-type electrochemical energy storage station in China so far. The topology of the 16 MW/71 MWh BESS in the

first stage of the Zhangbei national demonstration project is shown in Fig. 1. As can be seen, the wind/PV/BESS hybrid power generation system consists of a 100 MW wind farm, a 40 MW PV power station, a 14 MW/63 MWh lithium-ion BESS, a 2 MW/8 MWh redox flow BESS, and a power grid. The wind farm, PV power station and BESS are connected to the power grid through transformers. Specifically, the 14 MW/63 MWh lithium-ion BESS includes nine units (C001 to C009) in parallel (as shown in Table 1), each connected to a 35 kV AC bus by means of a 380 V/35 kV transformer unit. The topology of each lithium-ion BESS connected to the power grid is shown in Fig. 2. As indicated, each BESS contains multiple lithium-ion battery energy storage units in parallel, each unit consisting of a 500 kW power converter system (PCS) and multiple lithium-ion battery packs. Currently the large lithium-ion electrochemical energy storage station contains 46 sets of PCS and around 275000 lithium battery single cells. The lithium-ion battery energy storage unit can be controlled by using the PCS for management of start/stop and charging/discharging functions, etc.

The redox flow BESS, meanwhile, includes two sets of 1 MW/4 MWh redox flow sub-BESS (C010 to C011) in parallel, each connected to a 35 kV AC bus by means of a 380 V/35 kV transformer unit.

3 Key technologies for large battery energy storage systems

The key BESS technologies includes system integration and access, monitoring and control, energy management and application, and other aspects.

3.1 Structure and function of supervisory control & data acquisition system for BESS

The supervisory control and data acquisition (SCADA) system is the core component of battery energy storage power station, by which centralized access, real-time control and operation scheduling are achieved. More specifically, it is utilized to send information to and accept information from BESS equipment such as local control monitoring system and PCS, as well as to conduct real-time monitoring and carry out control management functions.

The SCADA structure proposed in this paper is illustrated in Fig. 3. As can be seen, a hierarchical distributed control scheme for BESS mainly includes three layers, namely, the master station layer, the local control and monitoring system (CMS) layer, and the device layer. The master station layer includes servers, workstations, and coordinated controllers. In the local CMS layer, there are eleven local controllers, and each is used to manage four or

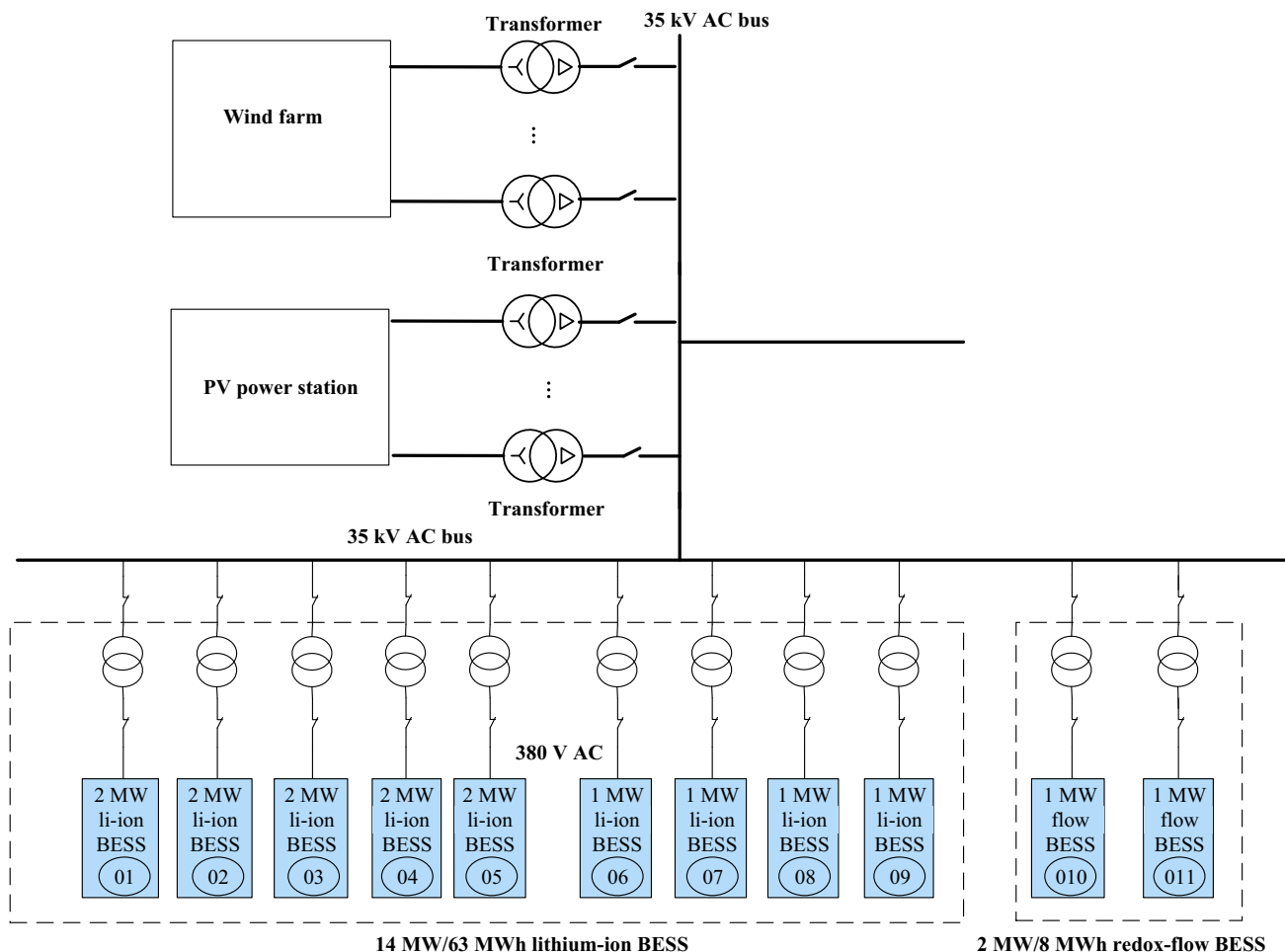


Fig. 1 Wind/PV/BESS hybrid power generation system

Table 1 System integration and components for BESS

Unit name	System integrator	Battery supplier	Battery management system (BMS) supplier	PCS supplier	Total capacity (MWh)	Unit capacity (MWh)	Unit maximum power (MW)	PCS rated power (kW)	PCS amount (set)
C001, C002, C003	CALB	CALB	PowerWise	SIFANG	9	3	2	500	12 (=4 × 3)
C004	WANXIANG	WANXIANG	WANXIANG	XJ	2	2	2	500	4 (=4 × 1)
C005, C006	ATL	ATL	ATL	SOARING	16	8	3	500	12 (=6 × 2)
C007, C008, C009	BYD	BYD	BYD	BYD	36	12	3	500	18 (=6 × 3)
C010, C011	Prudent Energy	Prudent Energy	Prudent Energy	ABB	8	4	1	500	10 (=5 × 2)

six PCS devices. In the device layer, there are PCS, battery devices, and power distribution cabinets.

Between these layers, information transmission is implemented via 100 Mbit/1000 Mbit fiber ring networks,

and is realized by means of a dual network communication system combining a monitoring network with a control network, as shown in Table 2. The functions of each layer are shown as follows.

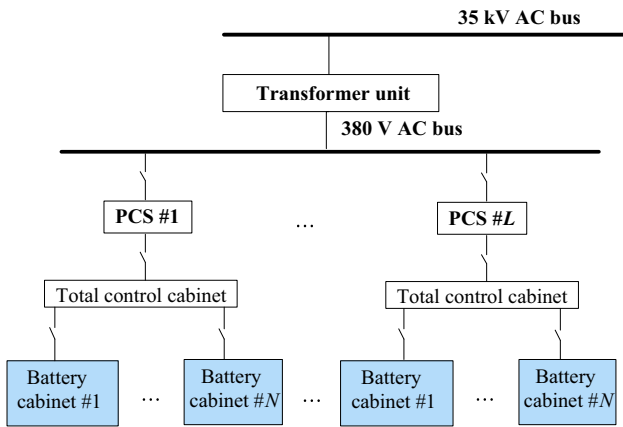


Fig. 2 Topology for sub-BESS under transformer unit

1) Master station layer

Master station layer is mainly responsible for coordinated control and energy management, communication management, data acquisition, data processing and management. It calculates power commands of transformer unit

stations by coordinated control and energy management system. Some key real-time running state data and control commands have been interactive between master station layer and local CMS layer through control network by using an Ethernet for plant automation (EPA) protocol based strong real-time Ethernet.

Detail running data of each transformer unit, including all single battery voltage, single battery temperature, and detailed operation information etc, have been transmitted from supplier local monitoring system to master station layer through IEC60875-5-104 (IEC-104) protocol based monitoring network.

The local controllers assign the target power to each associated PCS, to control the power of each PCS according to transformer-unit-based sub-BESS. The sub-BESS is distinguished based on 380 V/35 kV transformer unit.

Some key real-time running state data of BESS have been uploaded to the remote dispatch station center based on IEC-104 protocol.

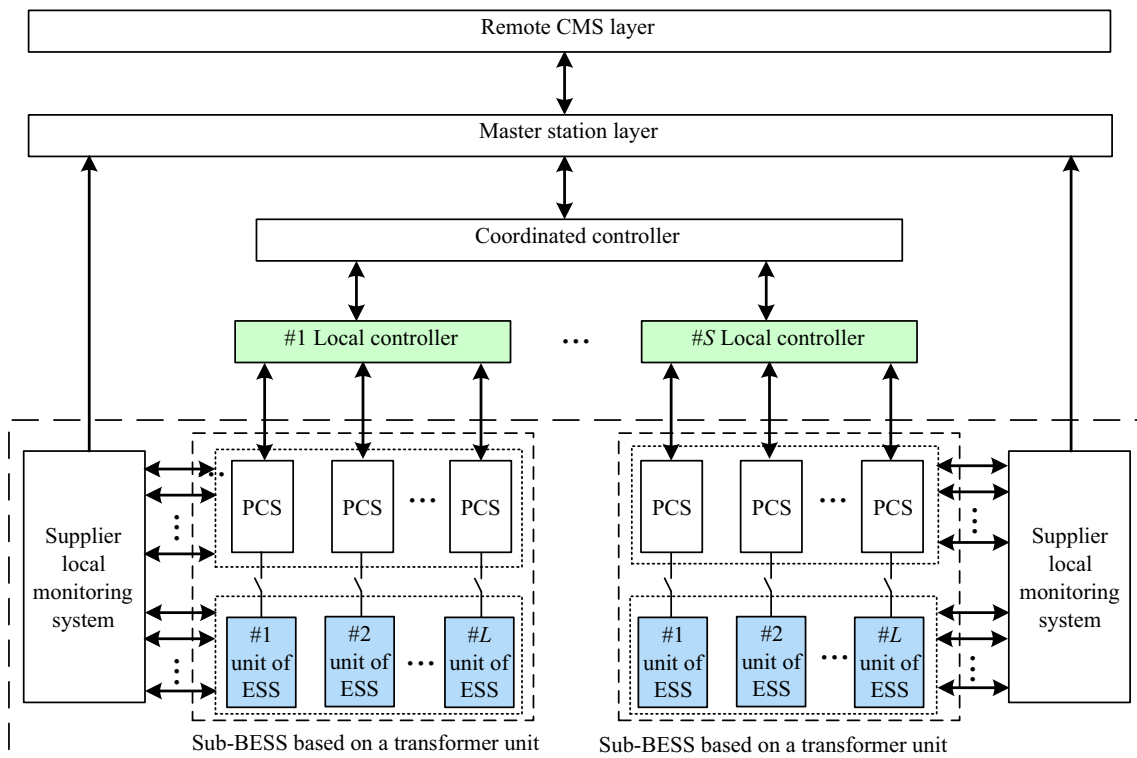


Fig. 3 Hardware platform structure of SCADA

Table 2 Communication protocol between the parts

Layers	Supplier local monitoring system	Local controller	Remote CMS layer
Master station layer	IEC-104	EPA	IEC-104
PCS layer	CAN	Modbus	-

2) Local CMS layer

The local CMS consists of three parts: the local controllers, the I/O stations, and the local monitoring system of supplier. The local controllers are used to receive commands from the coordination controller and, thus, to achieve regional-level (380 V voltage level) coordination control; the I/O stations convert the protocol of the converter interface, collects data and sends control commands. The local controllers monitors the BESS in real-time by using the VxWorks embedded operating system. Additionally, at the local CMS layer, the PCS, battery and distribution-system operational statuses are monitored in real-time, and the upper-layer control instructions are promptly send to each control PCS unit. Overall, this hierarchical control system effectively guarantees the control precision and stability of the storage system.

3) Device layer

The device layer contains a number of energy storage systems. For instance, a 500 kW/2 MWh energy storage system incorporates a 500 kW PCS, a 2 MWh energy storage battery unit and some BMSs. The PCS is mainly used to control the charge/discharge power and manage protection functions. The BMS is mainly used to manage the operation and control of the 2 MWh energy storage battery. Its main functions include the analog signal measurement, running battery system alarm, battery system protection, self-diagnostics, battery-balanced management, statistical storage, charge-discharge management, hypertension management, thermal management, communication, insulation testing, and others. The typical topology of the BMS is shown in Fig. 4.

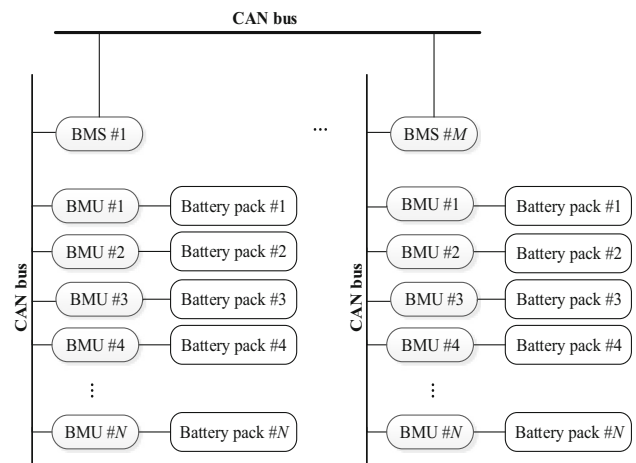


Fig. 4 Schematic diagram of typical topological structure of battery management system

3.2 Energy management system for large-scale BESS

Firstly, the work specification of the energy management system (EMS) for large-scale BESS has been designed as shown in Fig. 5. In the charge status, power is less than zero; and in the discharge status, power is greater than zero. The PCS is used to achieve the power and energy balance. The principles of the energy management supervision, in this paper, have been proposed according to the following objectives and constraints.

- 1) Objectives: To meet the real-time power requirement; To ensure the energy balance and availability.
- 2) Constraints: The limit of allowable maximum charge/discharge power; The limit of the charge/discharge capacity.

In this paper, a two level EMS has been proposed. One is main-EMS layer for transformer units in the station control layer. The other is sub-EMS layer for PCS units in the local CMS layer.

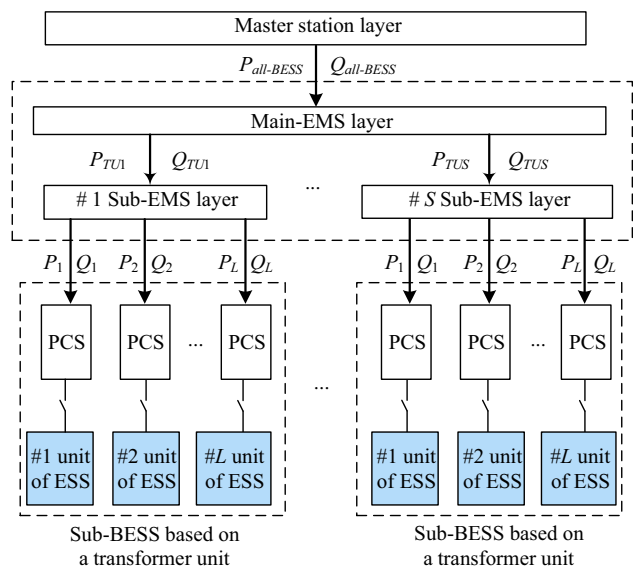


Fig. 5 EMS structure for BESS

The main-EMS, according to current collection status information of each transformer unit, calculates the power commands in real-time based on BESSs' total power demand, so as to prevent excess charge or excess discharge of the batteries. In accordance with the total power allocation strategy for a transformer unit, the sub-EMS allocates the transformer unit demand power to each PCS unit according to the status of PCS unit. The status parameters include the allowable maximum charge/discharge power of the PCS unit, and the state of charge (SOC), etc. And then real-time demand power is guaranteed to prevent over-charge/discharge of the battery, ensuring the safety and reliability of the transformer unit. The flow chart of the proposed EMS algorithm is shown in Fig. 6 and that is described in detail in the following sections respectively.

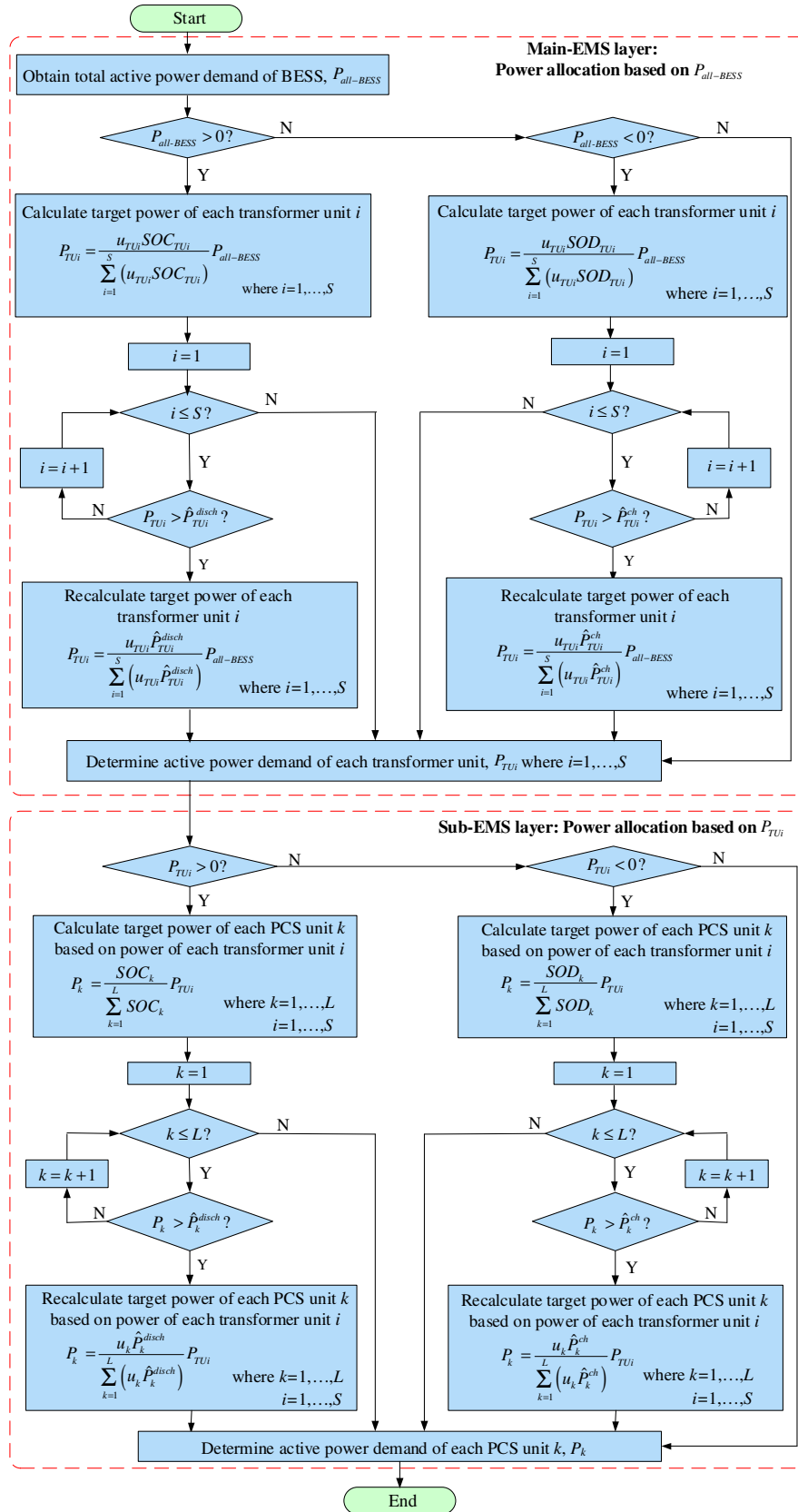


Fig. 6 Flow chart of the proposed EMS algorithm for active power control

3.2.1 Energy management strategy of main-EMS

Total active power demand of BESS, $P_{all-BESS}$, comes from the master station layer as shown in Fig. 5. The target power of each transformer unit i , P_{TU_i} , is calculated according to the allowable charging and discharging power and SOC. The purpose of this energy management step is to regulate the SOC for each transformer unit at an appropriate level during regulation while ensuring that the operational constraints such as charge/discharge power and battery SOC are not violated.

1) In the discharging status (when $P_{all-BESS} > 0$): P_{TU_i} is calculated by considering the SOC under each transformer unit i , SOC_{TU_i} and allowable maximum discharge power, $\hat{P}_{TU_i}^{disch}$ under each transformer unit i . Specific calculation steps are as follows.

Firstly, the initial target power of each transformer unit is calculated by using (1).

$$P_{TU_i} = \frac{u_{TU_i} SOC_{TU_i}}{\sum_{i=1}^S (u_{TU_i} SOC_{TU_i})} P_{all-BESS} \tag{1}$$

Secondly, if $P_{TU_i} > 0$ and $P_{TU_i} > \hat{P}_{TU_i}^{disch}$, P_{TU_i} calculated by (1) is determined again by using (2) and (3) based on the current allowable discharge power constraint for each transformer unit.

$$P_{TU_i} = \frac{u_{TU_i} \hat{P}_{TU_i}^{disch}}{\sum_{i=1}^S (u_{TU_i} \hat{P}_{TU_i}^{disch})} P_{all-BESS} \tag{2}$$

$$\hat{P}_{TU_i}^{disch} = \sum_{k=1}^L u_k \hat{P}_k^{disch} \tag{3}$$

where $P_{all-BESS}$ is the total active power demand of BESS; TU is representing the transformer unit; u_{TU_i} is the start-stop status under transformer unit i ; P_{TU_i} is the active power of transformer unit i ; $\hat{P}_{TU_i}^{disch}$ is the allowable maximum discharge power of transformer unit i ; u_k is the start-stop status of PCS k ; \hat{P}_k^{disch} is the allowable maximum discharge power of PCS k ; S is the total number of transformer unit; L is the total number of PCS for each transformer unit.

2) In the charging status (when $P_{all-BESS} < 0$): P_{TU_i} is calculated considering the stage of discharge (SOD) under each transformer unit i , SOD_{TU_i} , and allowable maximum charge power under each transformer unit i , $\hat{P}_{TU_i}^{ch}$. Specific calculating steps are as follows. Firstly, the target power of each transformer unit is calculated by using (4).

$$P_{TU_i} = \frac{u_{TU_i} SOD_{TU_i}}{\sum_{i=1}^S (u_{TU_i} SOD_{TU_i})} P_{all-BESS} \tag{4}$$

Secondly, if $P_{TU_i} < 0$ and $|P_{TU_i}| > |\hat{P}_{TU_i}^{ch}|$, P_{TU_i} is determined again by using (5) and (6) as follows based on the current allowable charge power constraint for each transformer unit.

$$P_{TU_i} = \frac{u_{TU_i} \hat{P}_{TU_i}^{ch}}{\sum_{i=1}^S (u_{TU_i} \hat{P}_{TU_i}^{ch})} P_{all-BESS} \tag{5}$$

$$\hat{P}_{TU_i}^{ch} = \sum_{k=1}^L u_k \hat{P}_k^{ch} \tag{6}$$

where $\hat{P}_{TU_i}^{ch}$ is the allowable maximum charge power of transformer unit i ; \hat{P}_k^{ch} is the allowable maximum charge power of PCS k ; S is the total number of transformer unit; L is the total number of PCS for each transformer unit.

3) In addition, in the discharging and charging status, the u_{TU_i} and SOC_{TU_i} is determined as follows. SOC_{TU_i} is generally calculated by (7).

$$SOC_{TU_i} = \frac{\left(\sum_{k=1}^L u_k SOC_k \right)}{\sum_{k=1}^L u_k} \tag{7}$$

$$SOD_{TU_i} = 1 - SOC_{TU_i} \tag{8}$$

If the SOC deviation between the controlled PCS units in the transformer unit is larger (this deviation can be determined based on the actual operation requirements), take the maximum SOC_k or minimum SOC_k as the SOC of transformer unit i according to the charge or discharge power needed.

3.2.2 Energy management strategy of sub-EMS

The target active power under each transformer unit, P_{TU_i} , comes from the main-EMS layer as shown in Fig. 6. The initial target power of each PCS is calculated using (9) and (11) below, and is then modified based on the allowable maximum charge/discharge capacity. Specific calculation steps are as follows.

1) In the discharging status (when $P_{TU_i} > 0$): P_i is calculated by the SOC of each PCS i , SOC_i and allowable maximum discharge power, \hat{P}_i^{disch} of each PCS i . That is, firstly, the initial target power of PCS i is calculated by (9).



$$P_i = \frac{SOC_i}{\sum_{i=1}^L SOC_i} P_{TUi} \tag{9}$$

Secondly, if $P_i > 0$ and $P_i > \hat{P}_i^{disch}$, P_i calculated by (9) is determined again by using (10) based on the current allowable discharging power constraint for each PCS unit.

$$P_i = \frac{u_i \hat{P}_i^{disch}}{\sum_{i=1}^L (u_i \hat{P}_i^{disch})} P_{TUi} \tag{10}$$

where u_i is the start-stop status of PCS i ; SOC_i is the SOC of PCS i .

2) In the charging status (when $P_{TUi} < 0$): P_i is calculated by the SOD of each PCS i , SOD_i and allowable maximum charge power, \hat{P}_i^{ch} of each PCS i . Firstly, the initial target power of PCS i is calculated based on the SOD of each PCS unit using (11) and (12) as follows.

$$P_i = \frac{SOD_i}{\sum_{i=1}^L SOD_i} P_{TUi} \tag{11}$$

$$SOD_i = 1 - SOC_i \tag{12}$$

where SOD_i is SOD of PCS i .

Secondly, if $P_i < 0$ and $|P_i| > |\hat{P}_i^{ch}|$, P_i is determined again by using (13) based on the current allowable charge power constraint of each PCS unit.

$$P_i = \frac{u_i \hat{P}_i^{ch}}{\sum_{i=1}^L (u_i \hat{P}_i^{ch})} P_{TUi} \tag{13}$$

3.2.3 Reactive power control strategy for BESS

The dynamic reactive power support function is one of the important applications of large-scale BESS. Typically, the storage control unit is in active power control mode. However, depending on the voltage regulation requirements, PCS units can provide dynamic reactive power support to the connected grid, in the form of reactive power compensation. A multi-level reactive power control strategy for BESS has been proposed based on maximum allowable reactive power level of each PCS. That is, the first-level control layer is the reactive power control between various energy storage transformer units, the second-level control layer is the reactive power control of each storage unit inside the transformer between the PCSs. The specific control method is explained below.

1) Reactive power control for each transformer unit

Total reactive power requirement of BESS, $Q_{all-BESS}$, comes from the master station layer as shown in Fig. 6. The purpose of this coordinated control step for reactive

power is to allocate the reactive power demand appropriately based on the reactive power supply capacity of each transformer unit. Then the reactive power under each transformer unit i , Q_{TUi} , is calculated by allowable maximum reactive power under each transformer unit i , \hat{Q}_{TUi} as shown in (14).

$$Q_{TUi} = \frac{u_{TUi} \hat{Q}_{TUi}}{\sum_{i=1}^L (u_{TUi} \hat{Q}_{TUi})} Q_{all-BESS} \tag{14}$$

where \hat{Q}_{TUi} is calculated based on the maximum allowable apparent power of PCS i , \bar{S}_i and the current active power of each PCS, P_i , are as shown in (15).

$$\hat{Q}_{TUi} = \sum_{i=1}^S \sqrt{\bar{S}_i^2 - P_i^2} \tag{15}$$

2) Reactive power control for each PCS unit

The real-time reactive power calculation method for each PCS proceeds as follows, based on the reactive power demand of each transformer unit.

The reactive power under each transformer unit, Q_{TUi} , comes from the main-EMS layer as shown in Fig. 6. The reactive power of each PCS is calculated based on the allowable maximum reactive power for PCS i , \hat{Q}_i , are as shown in (16).

$$Q_i = \frac{u_i \hat{Q}_i}{\sum_{i=1}^L (u_i \hat{Q}_i)} Q_{TUi} \tag{16}$$

where \hat{Q}_i is calculated by (17).

$$\hat{Q}_i = \sqrt{\bar{S}_i^2 - P_i^2} \tag{17}$$

4 Operational status of large BESS in China national demonstration project

4.1 Power generation tracking plan

The output power of wind farm in Zhangbei national renewable generation demonstration station is limited by regional dispatching system, but there is no output power restriction on the PV power generation. When the output power of wind farm is limited, the wind/PV/BESS hybrid system can be operated in the “tracking dispatch schedule output” mode.

Under conditions including strong winds, the wind farm output power increases in Zhangbei area, which may threaten the stability and security of the power grid. The BESS adjusts the power output according to the dispatched wind power generation schedule, so that the maximum

power is absorbed and wind power curtailment is reduced, by implementing the “tracking power schedule output” mode at the specified time.

Figure 7 shows the operation status for tracking power generation plan of 80 MW. By implementing the “tracking power schedule output” mode in the EMS, the deviation between the actual wind/PV power and the plan is effectively reduced, and the wind/PV/BESS hybrid system output power is restricted within the planned power range, thus meeting the “tracking power schedule output” mode’s requirements. Figure 8 shows power profiles of each transformer unit and total BESS. As shown in Fig. 8, olive curve is power of total BESS. Larger version of each transformer unit power is shown in Fig. 9.

By implementing EMS, the power of each transformer unit is effectively determined according to the allowable charging and discharging power ability and SOC. In the demonstration project, the allowable range of the battery SOC is usually set between 20% and 80%. Under this mode, the depth of discharge of the energy storage system is generally within 60%.

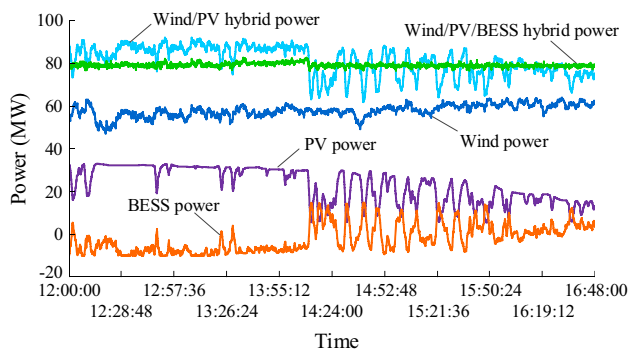


Fig. 7 Power generation tracking plan

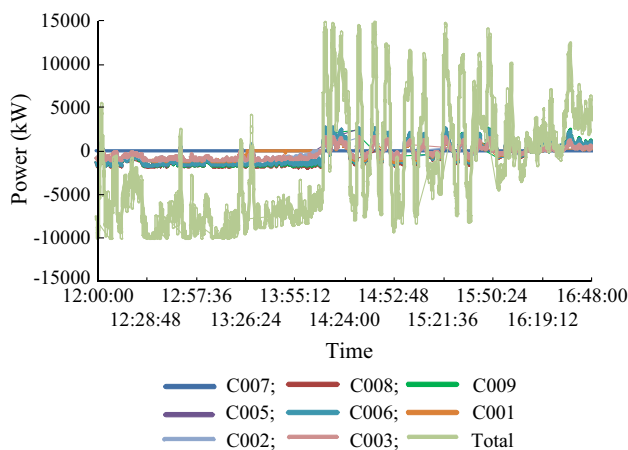


Fig. 8 Power profiles of each transformer unit and total BESS

4.2 Reactive power compensation

Figure 10 shows the test result for tracking reactive power plan by using BESS. The blue curve is target and the red curve is actual reactive power.

Based on the reactive power demand instructions sent by the master station, the total reactive power of the BESS can effectively follow the dispatched reactive power and its response speed meets the application requirements for voltage regulation. This reactive power compensatory utility has been applied in practice to the 16 MW BESS.

5 Technical benefits of system

The technical benefits of the BESS are reflected in many aspects.

1) Improvement of friendliness of renewable energy generation connected to the grid: The power fluctuations of renewable generation (such as wind and PV generations)

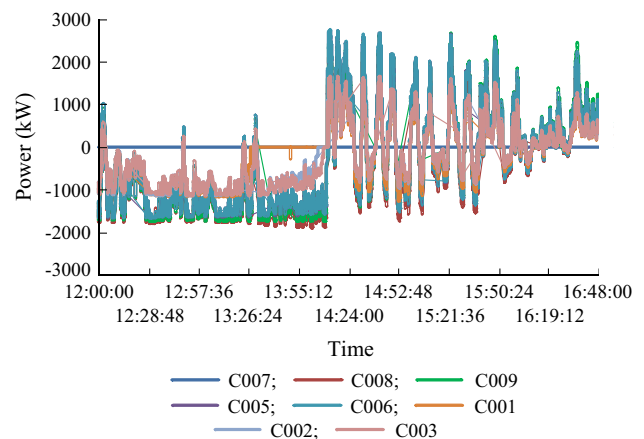


Fig. 9 Larger version of each transformer unit power

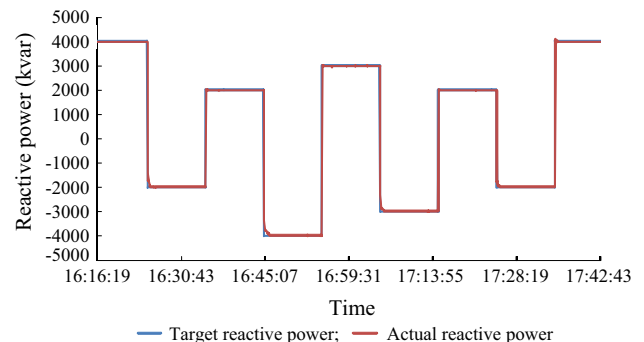


Fig. 10 Control effect of tracking reactive power command



under different time scales has posed great influences on the requirement of grid reserve, generation scheduling, security operations, and other aspects. Therefore, the China's national standards for wind power connected to the grid demand that the maximum power fluctuations of wind farms on different time scales should satisfy different technical indicators. Application of wind/PV/BESS hybrid power generation can effectively stabilize wind power fluctuation, help to reduce the impact of wind and PV power fluctuations on the grid, improve the grid stability, and create a better environment for grid integrations of large-scale wind farm and PV power station.

2) Wind power curtailment: In March 2012, China's National Energy Administration urged the provinces (cities) to strictly implement wind power project approval plans. In principle, new wind power project construction for a region shall not be arranged if the wind power curtailment is more than 20% of the total wind power to be generated. Wind power curtailment will not only affect the level of wind power development and the utilization of clean energy, but also will reduce the wind farm investment income. Application of an energy storage system can coordinate a grid to accommodate wind power maximally. Furthermore, energy storage device can absorb the renewable generation in "off peak" load period, and conduct the peak shaving in "peak" load period. This will effectively not only increase the wind power accommodation level in the grid, but also reduce the curtailment of wind power.

3) Reactive power compensation: Wind and PV power generation can easily cause bus voltage fluctuation, even beyond the voltage limit. Such fluctuation, when serious, will affect the voltage stability of the power grid. The demonstration project's BESS can provide reactive power support according to a reactive power dispatch plan. As a result, the BESS can assist other reactive power compensation equipment to control the bus voltage at an expected level and reduce voltage fluctuations and flickers, and ensuring, thereby, the voltage stability of the grid connected with wind and PV farms.

4) Improvement of dynamic characteristic of power grid: The response speed of traditional frequency regulation unit is relatively slow, and the ramp rate is low. Thus, it cannot fully meet the needs of new frequency stability problems caused by the rapid development of the grid connected with large renewable generation. By utilization of the characteristics of both fast response and strong short-term power handling capacity of BSEE, more benefits can be obtained through flexible control of BSEE to participate in power grid frequency regulation. This will help maintain the system frequency within the standard range and improve power grid security and system stability.

6 Conclusion

In this paper, the system configuration of China's national demonstration project which has mixed various generations, such as wind, PV, and BESS together with a power transmission system is introduced, and the key technologies and operation status of large-scale battery energy storage system have been presented. Moreover, the benefits of such a large BESS in dealing with the fluctuation and intermittence of large renewable generation and improving the operation stability for transmission grid, etc., are discussed. Overall content is summarized as follows.

1) The coordinated control and monitoring of large-scale BESS including around 275000 single cells of lithium-ion battery can be realized effectively. The control response time of the BESS can be achieved within second level and this meets the actual operational requirements for the BESS.

2) The key issues for coordinated control and energy management of large-scale BESS can be solved by the proposed EMS combined with local controllers and coordinated control architecture.

3) A variety of applications for large BESS have been implemented and achieved including tracking power generation plan and reactive power compensation etc. Through demonstration it has been verified that the controllability and schedulability for wind farm and PV power station can be improved effectively by using proposed control systems.

4) Battery energy storage technology has some technical benefits, however, the high cost of BESS is currently indeed a problem which cannot be ignored. In order to more efficient use the BESS, the further R&D and verification associated with the operation and application technologies of the large-scale BESS need to be continued based on the demonstration project.

Acknowledgment This work was supported by National Natural Science Foundation of China (No. 51107126 and No. 512111046), the Key Projects in National Science and Technology Pillar Program (No. 2011BAA07B07), the Beijing Nova Program (No. Z141101001814094), and the Science and Technology Foundation of State Grid Corporation of China (No. DG71-14-032).

Open Access This article is distributed under the terms of the Creative Commons Attribution 4.0 International License (<http://creativecommons.org/licenses/by/4.0/>), which permits unrestricted use, distribution, and reproduction in any medium, provided you give appropriate credit to the original author(s) and the source, provide a link to the Creative Commons license, and indicate if changes were made.

References

- [1] Li XJ, Hui D, Lai XK (2013) Battery energy storage station (BESS)-based smoothing control of photovoltaic (PV) and wind power generation fluctuations. *IEEE Trans Sustain Energy* 4(2):464–473

- [2] Toge M, Kurita Y, Iwamoto S (2013) Supplementary load frequency control with storage battery operation considering SOC under large-scale wind power penetration. In: Proceedings of the 2013 IEEE Power and Energy Society general meeting, Vancouver, Canada, 21–25 Jul 2013, 5 pp
- [3] Kawakami N, Iijima Y, Fukuhara M et al (2010) Development and field experiences of stabilization system using 34 MW NAS batteries for a 51 MW wind farm. In: Proceedings of the 2010 IEEE international symposium on industrial electronics (ISIE'10), Bari, Italy, 4–7 Jul 2010, pp 2371–2376
- [4] Khatamianfar A, Khalid M, Savkin AV et al (2013) Improving wind farm dispatch in the Australian electricity market with battery energy storage using model predictive control. *IEEE Trans Sustain Energy* 4(3):745–755
- [5] Teleke S, Baran ME, Huang AQ et al (2009) Control strategies for battery energy storage for wind farm dispatching. *IEEE Trans Energy Convers* 24(3):725–732
- [6] Baccino F, Grillo S, Marinelli M et al (2011) Power and energy control strategies for a vanadium redox flow battery and wind farm combined system. In: Proceedings of the 2nd IEEE PES international conference and exhibition on innovative smart grid technologies (ISGT Europe'11), Manchester, UK, 5–7 Dec 2011, 8 pp
- [7] Li WY (2015) Framework of probabilistic power system planning. *CSEE J Power Energy Syst* 1(1):1–8
- [8] Nguyen CL, Lee HH (2016) Effective power dispatch capability decision method for a wind-battery hybrid power system. *IET Gener Transm Distrib* 10(3):661–668
- [9] Haaren RV, Morjaria M, Fthenakis V et al (2015) An energy storage algorithm for ramp rate control of utility scale PV (photovoltaics) plants. *Energy* 91:894–902
- [10] Wang GS, Ciobotaru M, Agelidis VG (2014) Power smoothing of large solar PV plant using hybrid energy storage. *IEEE Trans Sustain Energy* 5(3):834–842
- [11] Yuan Y, Sun CC, Li MT et al (2015) Determination of optimal supercapacitor-lead-acid battery energy storage capacity for smoothing wind power using empirical mode decomposition and neural network. *Electr Power Syst Res* 127:323–331
- [12] Trung TT, Ahn SJ, Choi JH et al (2014) Real-time wavelet-based coordinated control of hybrid energy storage systems for denoising and flattening wind power output. *Energies* 7(10):6620–6644
- [13] Abbey C, Strunz K, Joós G (2009) A knowledge-based approach for control of two-level energy storage for wind energy systems. *IEEE Trans Energy Convers* 24(2):539–547
- [14] Shigematsu T (2011) Redox flow battery for energy storage. *SEI Tech Rev* 73:4–13
- [15] Senjyu T, Kikunaga Y, Yona A et al (2008) Coordinate control of wind turbine and battery in wind power generator system. In: Proceedings of the 2008 IEEE Power and Energy Society general meeting—conversion and delivery of electrical energy in the 21st century, Pittsburgh, PA, USA, 20–24 Jul 2008, 7 pp
- [16] Ferreira SR, Rose DM, Schoenwald DA et al (2012) Protocol for uniformly measuring and expressing the performance of energy storage systems. PNNL-22010. Pacific Northwest National Laboratory, Richland, WA, USA
- [17] US utility-scale battery storage market surges forward. 2011NARP 825-110928. IHS Emerging Energy Research LLC, Cambridge, MA, USA
- [18] DOE global energy storage database. <http://www.energystorageexchange.org/projects>
- [19] Skyllas-Kazacos M, Kazacos G, Poon G et al (2010) Recent advances with UNSW vanadium-based redox flow batteries. *Int J Energy Res* 34(2):182–189
- [20] Yoshimoto K, Nanahara T, Koshimizu G (2006) New control method for regulating state-of-charge of a battery in hybrid wind power/battery energy storage system. In: Proceedings of the 2006 IEEE PES power systems conference and exposition (PSCE'06), Atlanta, GA, USA, 29 Oct–1 Nov 2006, pp 1244–1251
- [21] Viswanathan V, Kintner-Meyer M, Balducci P et al (2013) National assessment of energy storage for grid balancing and arbitrage, phase II volume 2: cost and performance. PNNL-21388 PHASE II/Vol 2. Pacific Northwest National Laboratory, Richland, WA, USA
- [22] Supra JD (2012) Washington energy update: August–September 2012. White & Case LLP, New York, NY, USA
- [23] Kumagai J (2012) A battery as big as the grid. *IEEE Spectrum* 49(1):45–46

Xiangjun LI received the B.E. degree in electrical engineering from Shenyang University of Technology, China, in July 2001, and the M.E. and Ph.D. degrees in electrical and electronic engineering from Kitami Institute of Technology (KIT), Japan, in March 2004 and March 2006, respectively. From May 2006 to March 2010, he worked as post-doctoral research fellow at Korea Institute of Energy Research (KIER), Daejeon, Korea, and Tsinghua University, Beijing, China, respectively. In March 2010, he joined Electrical Engineering and New Material Department, China Electric Power Research Institute (CEPRI), Beijing, China, where he has been engaged in the topic of integration/control/SCADA/application technologies for large-scale multi-type battery energy storage system/station, wind/PV/battery hybrid distributed generation systems, and micro-grids. His research interests include renewable energy power generation, electric energy saving/storage technology, and power system engineering. Dr. Li is a chartered engineer, and the senior members of IEEE, CSEE, CAS, and CES, etc. He has been the Editor-in-Chief for a Springer book series entitled “Renewable Energy Sources & Energy Storage” since 2016. He has served as the Chair of the IEEE CIS Task Force on “ADP and RL in Power and Energy Internets” since 2016. He also serves as several members, such as the IEC TC120 WG3, the IEEE CIS Adaptive Dynamic Programming and Reinforcement Learning Technical Committee, and the IEEE CIS Intelligent Systems Applications Technical Committee, respectively.

Liangzhong YAO received the M.Sc. and Ph.D. degrees in electrical power engineering from Tsinghua University, Beijing, China, in 1989 and 1993, respectively. He is currently the Vice President and the Doctoral Supervisor of the China Electric Power Research Institute (CEPRI). Prior to CEPRI, he was the Senior Power System Analyst at ABB UK Ltd from 1999 to 2004, and was the Department Manager for network solution and renewable energy at Alstom Grid Research & Technology Centre in the UK from 2004 to 2011. Dr. Yao is a Fellow of IET, a chartered engineer, and a member of CIGRE. He is also the visiting professor at the University of Bath in the UK, and the guest professor at both Shanghai Jiao Tong University and Sichuan University, China.

Dong HUI received his B.S. and M.S. degrees in semiconductor physics and devices from Huazhong University of Science and Technology, China in 1990 and 1995, and Ph.D. degree in applied superconductivity, from Institute of Electrical Engineering, Chinese Academy of Sciences, in 1998, respectively. He worked as visiting scientist at Deutsches Elektronen Synchrotron (DESY), Hamburg, Germany, from May 1999 to May 2002. After then, he worked as associate professor, at the Institute of Electrical Engineering, Chinese Academy of Sciences, from May 2002 to May 2007. He has been a professor at China Electric Power Research Institute since June 2007 and now the chief engineer of electrical engineering and new material department of CEPRI. His research interests include large scale battery energy storage and power electronics.

